A time-domain model for railway rolling noise

The Wheel

Vibration

Curved Waveguide Finite Element method
The curved *WFE* assumes harmonic oscillation around the circumference of the wheel. The FE system of equations

$$\left[\mathbf{K}_2(-j\kappa)^2 + \mathbf{K}_1(-j\kappa) + \mathbf{K}_0 - \omega^2\mathbf{M}\right]\mathbf{\Phi}(\kappa,\omega) = \mathbf{0}$$

is solved for each discrete wavenumber κ corresponding to the number of oscillations. This produces the eigenfrequencies ω_0 and mode shapes $\mathbf{\Phi}_l$ of the wheel. $\mathbf{K}$ and $\mathbf{M}$ are stiffness- and mass matrices. The figure below shows two modes of the wheel:

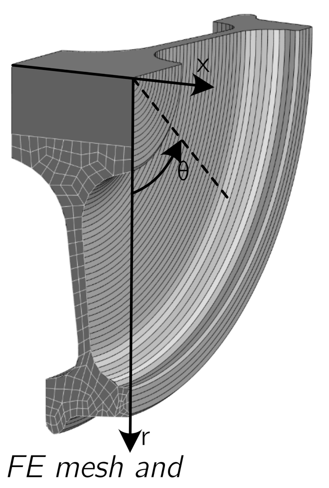

FE mesh and coordinate definition

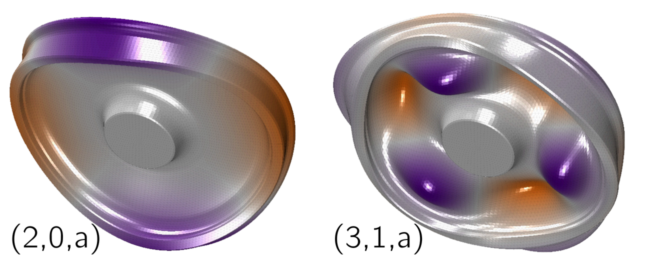

The velocity field $\mathbf{v}$ on the wheel due to an force $\mathbf{F}_e(\omega)$ is obtained by modal superposition,

$$\mathbf{v}(\theta,\omega) = \sum_l A_l(\omega)\mathbf{\Phi}_l$$

with the modal amplitude A_l

$$A_l(\omega) = j\omega b_l(\omega)\mathbf{F}_e(\omega)\mathbf{\Phi}_l(\mathbf{x}_0)$$

where

$$b_l(\omega) = \frac{1}{\Lambda_l(\omega_l^2 - \omega^2 + j2\omega\omega_l\zeta_l)}$$

and

$$\Lambda_l = \mathbf{\Phi}_l^{\mathrm{H}}\mathbf{M}\mathbf{\Phi}_l.$$

The surface velocity serves as the input to the boundary element model and to the wheel/rail interaction model.

Radiation

Fourier series Boundary Element method
The *FBEM* also makes use of the axisymmetry of the wheel by decomposing the sound field into a Fourier series. The BE problem reduces from 3D to 2D, however, now 2D BE problems are solved at each Fourier order. While FBEM is an efficient solution for predicting the sound field around a vibrating, stationary wheel, it is not convenient for simulating the pass-by of a wheel in time domain. Instead, an equivalent source model is used:

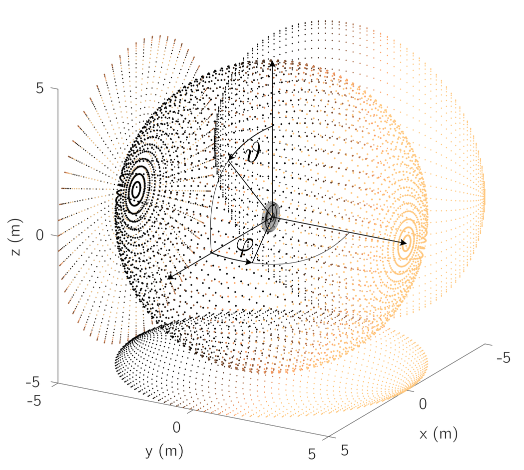

FBEM is used to evaluation the sound field on a sphere, which serves as input to the SH decomposition.

Spherical Harmonics
Representing the sound field by *SH* equivalent sources allows the efficient calculation of sound pressure transfer functions $H_l(x_\mathrm{S}, y_0, z_0, \omega)$ to any receiver position. SH decompositions are carried out for each mode l. The figures below show the directivity of the mode (3,1,a).

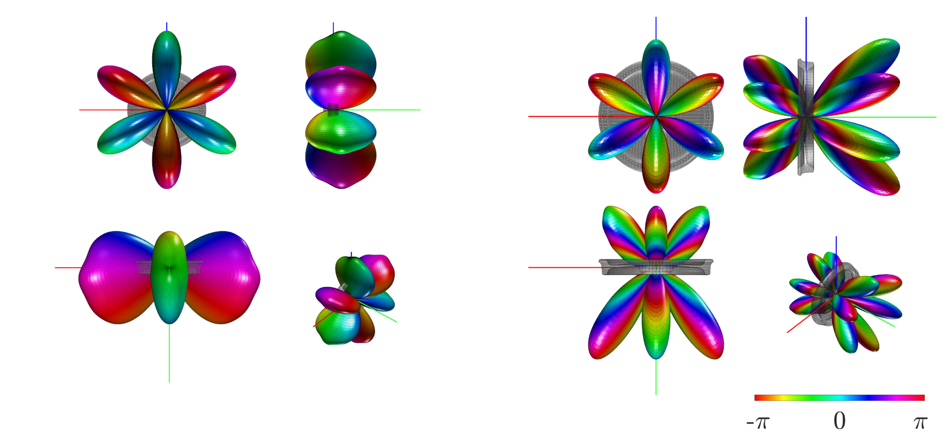

Pass-by noise

Modal pass-by prediction
Since the wheel is only very lightly damped, it has decay times of over 20 seconds. Calculating Green's functions which include the structural response is therefore not feasible in BEM/SH. Instead the structural response is separated from the acoustic radiation:

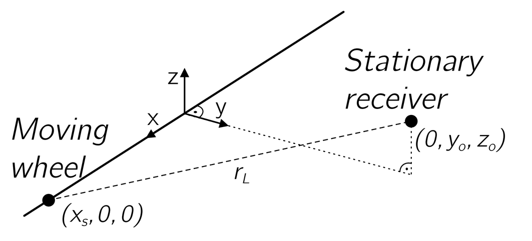

The modal amplitude $A_l(\omega)$ consists of the two terms $A_l(x_\mathrm{S},\omega) = F_{\mathrm{A},l}(\omega)b_l(\omega)$. $F_{\mathrm{A},l}(\omega)$ is expressed in time domain by differentiating $\mathbf{F}_e(\omega)$ and scaling with $\mathbf{\Phi}_l$. The term $b_l(\omega)$ describes the frequency response of an harmonic oscillator, for which an analytic expression exists:

$$b_l(t) = \frac{e^{-2\omega_l\zeta_l t}}{\Lambda_l\omega_l'}\sin(\omega_l' t)\mathrm{H}(t)$$

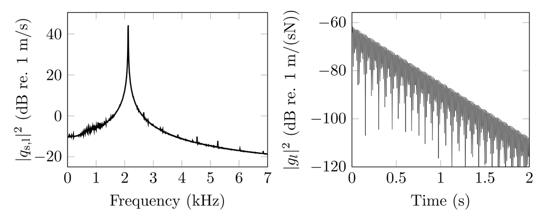

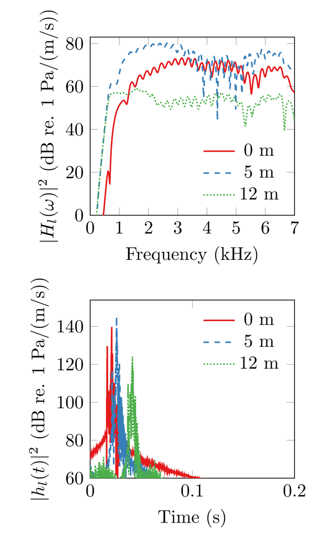

Convolution of $b_l(t)$ and $F_{\mathrm{A},l}(x_\mathrm{S}, t)$ gives the modal amplification $q'_{\mathrm{S},l}$

$$q'_{\mathrm{S},l}(x_\mathrm{S}, x_\mathrm{S}/v) = \int_{-\infty}^{x_\mathrm{S}/v} F_{\mathrm{A},l}(x_\mathrm{S},\tau)b_l(x_\mathrm{S}/v - \tau)\,\mathrm{d}\tau$$

Then, acoustic propagation functions $h_l(x_\mathrm{S}, t)$ from each mode are evaluated by inverse Fourier transform, and finally, convolution of $q'_{\mathrm{S},l}$ and h_l produces the pass-by pressure of mode l

$$p_l(t) = \int_{-\infty}^{\infty} q'_{\mathrm{S},l}(x_\mathrm{S}, x_\mathrm{S}/v)h_l(x_\mathrm{S}, t - x_\mathrm{S}/v)\mathrm{d}x_\mathrm{S}$$

The total pressure is then calculated as the sum of all modal contributions. The acoustic propagation functions are smooth in frequency domain, so they can be evaluated with a broad frequency spacing.

The Interaction

Contact

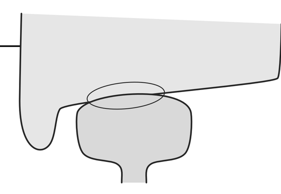

3D non-Hertzian, non-linear contact model
The contact model combines the information about the surface roughness of the wheel and the rail with the local geometry to predict shape and size of the contact area, local displacements and stresses.

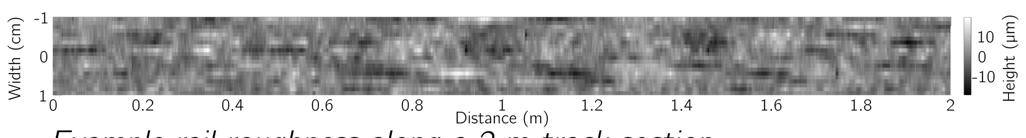

Example rail roughness along a 2 m track section

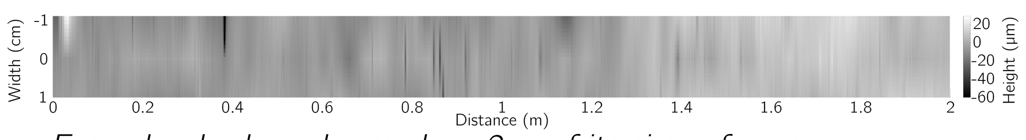

Example wheel roughness along 2 m of its circumference

Wheel and rail are locally approximated by an elastic half space. The potential contact area is discretised into rectangular elements. Each element influences each other element and a non-linear system of equations needs to be solved at each time step. Kalker's NORM and TANG algorithm are used to solve the normal and tangential problem, respectively.

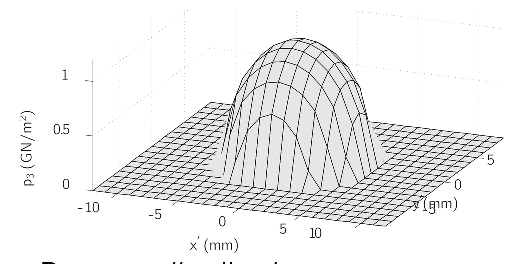

Pressure distribution in the contact zone.

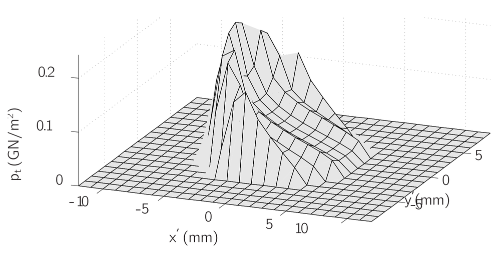

Total tangential stress in the contact zone.

Wheel/Rail interaction

Time-domain interaction: moving Green's functions
The wheel/rail interaction is efficiently solved in the time domain via moving Green's functions. The Green's functions are precalculated and contain the dynamic properties of the wheel, specifically the receptance at the contact point

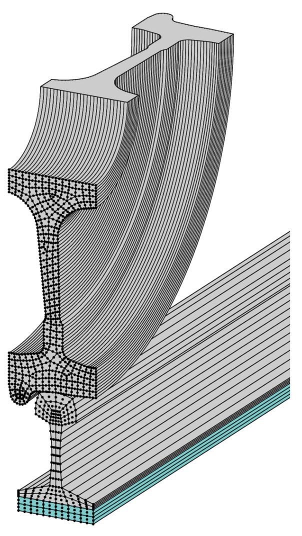

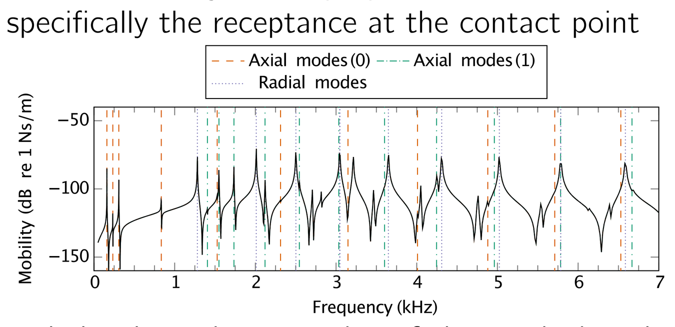

and the dynamic properties of the track, i.e. the receptance at the contact point on the rail

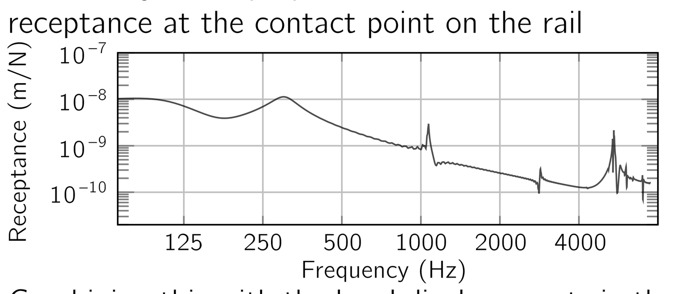

Combining this with the local displacements in the contact patch at every time step, the rolling contact forces can be calculated by convolution. This time-domain formulation allows including transient and non-linear effects such as wheel flats and curve squeal. The figure below shows an example time history of rolling contact forces.

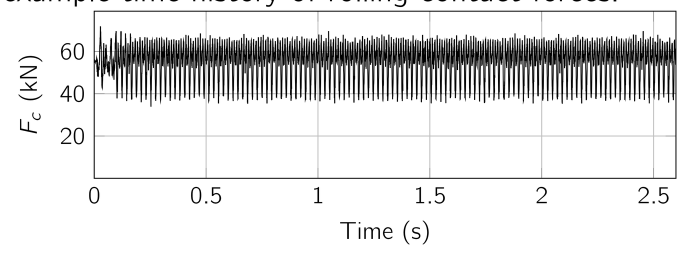

Results

Wheel pass-by noise in the time domain
The figure below shows a spectrogram of a single wheel passing by a stationary microphone position.

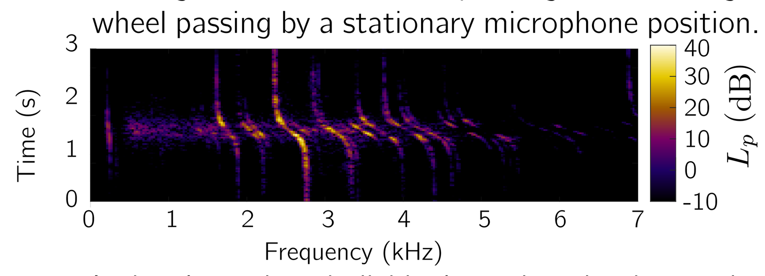

It is clear that individual modes dominate the spectrum, and the Doppler shift is visible. Modelling the pass-by noise radiated by each mode allows quantifying the contribution of each mode to the total sound pressure:

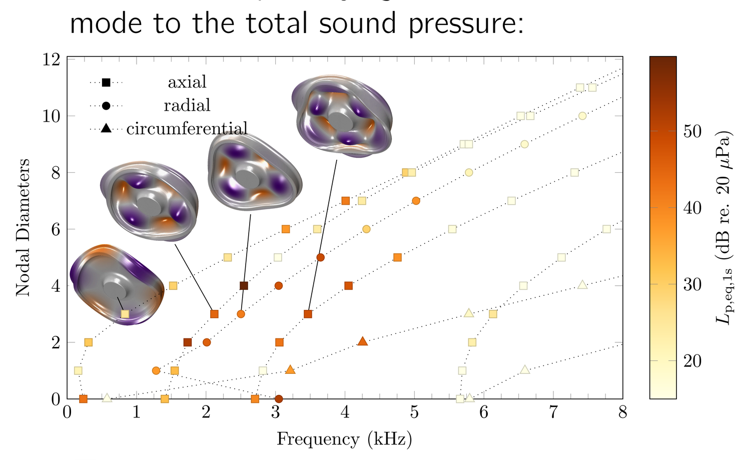

Track pass-by noise in the time domain
The figure below shows a spectrogram of force on the rail passing a stationary microphone position.

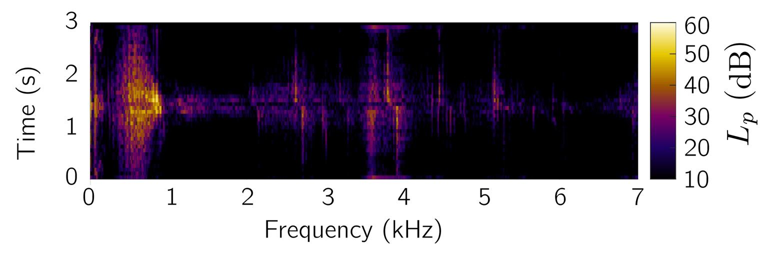

The track radiates noise mostly below 1 kHz. As above, the Doppler shift is visible.

The Track

Vibration

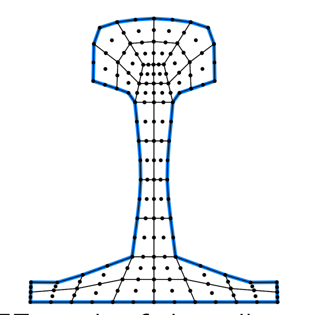

FE mesh of the rail. The velocity on the outer boundary is input to the radiation calculation.

Straight Waveguide Finite Element method
The WFE makes use of the constant cross-section along the track, assuming propagating, decaying waves in that dimension, which reduces the FE problem to 2D. The system of equations

$$\left[\mathbf{K}_2(-j\kappa)^2 + \mathbf{K}_1(-j\kappa) + \mathbf{K}_0 - \omega^2\mathbf{M}\right]\mathbf{\Phi}(\kappa,\omega) = \mathbf{0}$$

is solved by prescribing ω. This produces conjugate complex wavenumbers κ_i and cross-sectional modes $\mathbf{\Phi}_l$ of the rail:

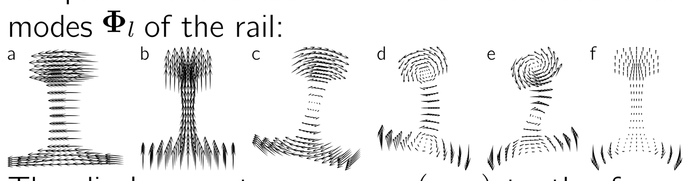

The displacement response $\mathbf{u}(x,\omega)$ to the force $\mathbf{F}_0(\kappa,\omega)$ is calculated by superposition of all waves,

$$\mathbf{u}(x,\omega) = \sum_i A_i\mathbf{\Phi}_{iR}e^{-j\kappa_i x} \text{ for } x \geq 0$$

with

$$A_i = \frac{j\mathbf{\Phi}_{nL}\mathbf{F}_0(\kappa,\omega)}{\mathbf{\Phi}_{nL}\mathbf{D}(\kappa_i)\mathbf{\Phi}_{iR}} \text{ and } \mathbf{D}(\kappa_i) = -2\kappa_i\mathbf{K}_2 - j\mathbf{K}_1$$

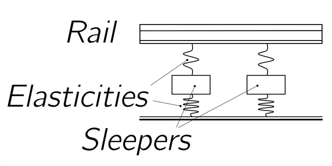

The *discrete support* of the rail is introduced by assuming that the displacement response is a superposition of the free rail response and the response due to the reaction forces,

$$u_{r,i} = \alpha_{r,ie}F_e - \sum_{l=1}^{N}\alpha_{r,il}F_{a,l}$$

and with $u_{r,i} = \alpha_{a,il}F_{a,i}$, a system of equations with the unknown reaction forces $\mathbf{F_a}$ can be set up and solved. The total displacement is then calculated by summing the displacements due to each force.

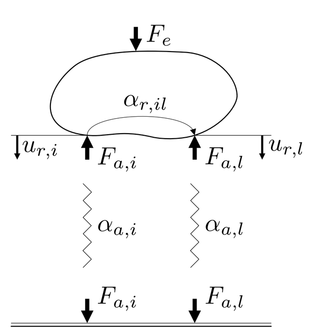

Radiation

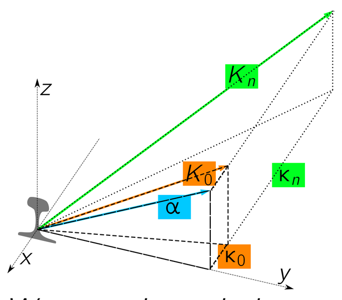

Wavenumber relations in WBEM

Wavenumber domain Boundary Element method
In the WBE, the 3D sound field (with the wavenumber in air K) is expressed as 2D sound fields (with in-plane wavenumber α) at each wavenumber κ along the track to reduces the computational cost. Numerical efficiency is further increased by

1. precalculating acoustic transfer functions H_a, i.e. the sound pressure produced at a set of receiver positions for a unit velocity at each boundary element:

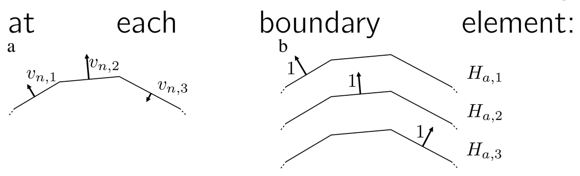

The total sound pressure is calculated by scaling and adding these functions.

2. re-using 2D BE solutions for a given α at different combinations of wavenumber κ and frequency (and thus K)

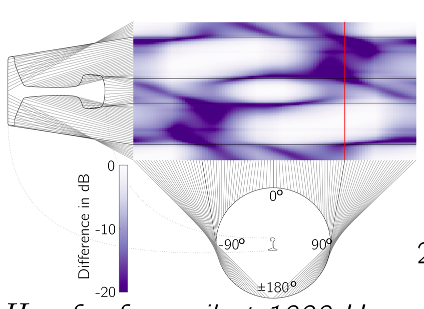

H_a of a free rail at 1000 Hz

Sound field radiated by discrete sleepers
The velocity profile $v_{n,i}$ of each sleeper along the track is expressed by Heaviside functions H

$$v_{n,i}(x,\omega) = v_{n,i}^*(\omega)\left(\mathrm{H}\left(x - id + \frac{w}{2}\right) - \mathrm{H}\left(x - id - \frac{w}{2}\right)\right)$$

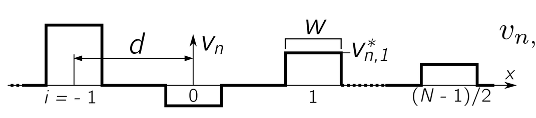

Sleeper velocity profile along the track.

which is conveniently expressed in wavenumber domain as $v_{n,i}(k,\omega) = v_{n,i}^*(\omega)\, w\, \mathrm{sinc}(\kappa w)\, \mathrm{e}^{-j\kappa id}$ and serves as the input to the WBEM.

Pass-by signals

Pass-by sound pressure via moving Green's functions
The figure below shows the frequency-wavenumber domain representation of the surface velocity of the rail and the sleepers.

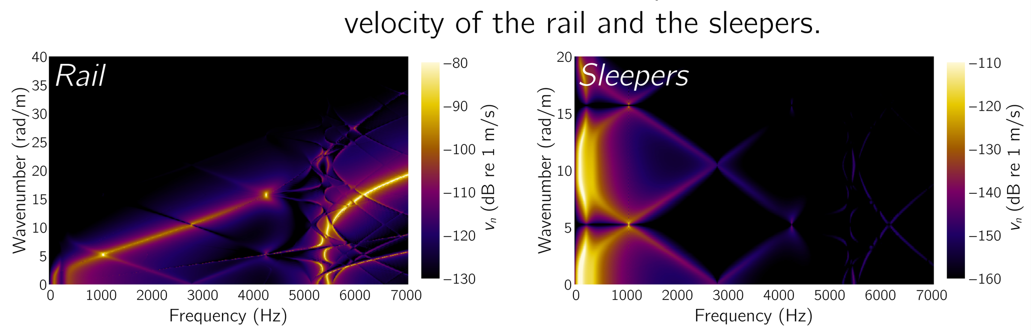

Multiplying the velocity of each surface element with its corresponding acoustic transfer function H_a and subsequent 2D inverse Fourier transform generates impulse responses describing the pressure response to a unit pulse along the track.

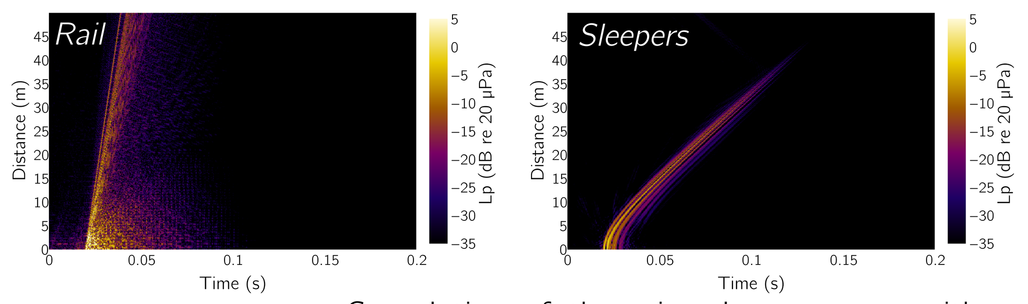

Convolution of these impulse responses with a rolling contact force allows calculating in the sound pressure in a track-side position in time-domain.

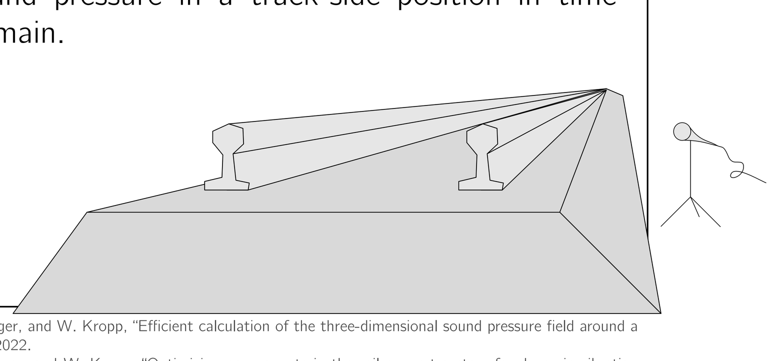

[1] J. Theyssen, "Simulating rolling noise on ballasted and slab tracks: vibration, radiation, and pass-by signals," Doctoral Thesis, Chalmers University of Technology, Gothenburg, Sweden, 2022.
[2] F. Fabre, J. S. Theyssen, A. Pieringer, and W. Kropp, "Sound radiation from railway wheels including ground reflections: A half-space formulation for the Fourier boundary element method," JSV, vol. 493, p. 115822, 2021.
[3] J. Theyssen, T. Deppisch, A. Pieringer, and W. Kropp: "On the efficient simulation of pass-by noise signals from railway wheels", Preprint, 2022.
[4] A. Pieringer, W. Kropp, and D. J. Thompson, "Investigation of the dynamic contact filter effect in vertical wheel/rail interaction using a 2D and a 3D non-Hertzian contact model," Wear, vol. 271, no. 1, pp. 328–338, May 2011.
[5] A. Pieringer, "Time-domain modelling of high-frequency wheel/rail interaction," Doctoral Thesis, Chalmers University of Technology, Gothenburg, Sweden, 2011.
[6] J. Theyssen, A. Pieringer, and W. Kropp, "The Influence of Track Parameters on the Sound Radiation from Slab Tracks," in Noise and Vibration Mitigation for Rail Transportation Systems, vol. 150, Cham, 2021.
[7] J. Theyssen, A. Pieringer, and W. Kropp, "Efficient calculation of the three-dimensional sound pressure field around a railway track.", Preprint, 2022.
[8] J. Theyssen, A. Pieringer, and W. Kropp, "Optimizing components in the rail support system for dynamic vibration absorption and pass-by noise reduction.", Contribution to the International Workshop on Railway Noise, Shanghai, 2022.

Jannik Theyssen, Astrid Pieringer, Wolfgang Kropp
jannik.theyssen@chalmers.se
Division of Applied Acoustics / CHARMEC
Chalmers University of Technology
Gothenburg, Sweden

CHALMERS
UNIVERSITY OF TECHNOLOGY